# DFT Study of the Reactions between Singlet-Oxygen and a Carotenoid Model

**Marco Garavelli,[†] Fernando Bernardi,*[,†] Massimo Olivucci,[†] and Michael A. Robb[‡]**

*Contribution from Dipartimento di Chimica "G. Ciamician", Università di Bologna, Via Selmi 2, 40126 Bologna, Italy, and Department of Chemistry, King's College, London, Strand, London, UK WC2R 2LS*

*Received February 17, 1998. Revised Manuscript Received July 6, 1998*

**Abstract:** Carotenoids such as $\beta$-carotene are one of the most efficient singlet-oxygen ($^1O_2$) quenchers. They quench *catalytically* $^1O_2$ (a highly reactive and toxic form of oxygen) through an almost diffusion-controlled energy transfer process (physical pathway): $^1O_2$ + carotenoid → $^3O_2$ + $^3$carotenoid → $^3O_2$ + carotenoid (+ heat) (eq 1). In contrast to physical quenching, less efficient but concomitant processes exist, involving real chemical reactions. For example, chemical oxidation reactions, which result in the destruction of carotenoids and thus in the loss of antioxidant protection, have been observed (chemical pathway): $^1O_2$ + carotenoid → chemical pathway (eq 2). To obtain more detailed information about the reactions between carotenoids and singlet-oxygen, we have performed a DFT computational study of the reaction mechanisms involved in the attack of $^1O_2$ to the *all-trans*-decaottanonaene (**$P_9$**), a polyene with 9 conjugated double bonds, chosen as carotenoid model. We have found that, together with the main energy transfer pathway (eq 1) which is almost barrierless, there are secondary but concomitant reactions (eq 2) with low-energy barriers leading to biradical intermediates via direct addition of $^1O_2$ to **$P_9$**. These biradicals may give ring closure to form 1,2-addition dioxetane products whose decomposition leads to the observed carbonyl chain cleavage oxidation fragments. However, these biradicals seem to be also responsible, through an $S_0 \rightarrow T_1$ *intersystem crossing*, of an alternative chemically mediated *catalytic* quenching of the singlet-oxygen which is returned to its triplet deactivated ground state through a dissociation process on $T_1$.

## 1. Introduction

Carotenoids are important plant pigments occurring inside photosynthetic systems where they exert the dual function of light harvesting (acting as accessory antenna pigments) and photoprotection (quenching singlet-oxygen $^1O_2$ and chlorophyll triplets)[1]. A protective action toward biological tissues has also been observed for unbound carotenoids (particularly $\beta$-carotene);[2] these properties may depend on carotenoid free radical-scavenging (antioxidant) activity as well as singlet-oxygen quenching activity.[3−8] Carotenoids are indeed one of the most efficient $^1O_2$ quenchers.[1,9] They quench $^1O_2$ *catalytically* (carotenoids are regenerated) through a very efficient (approaching the diffusion control limit) energy transfer process followed by an *intersystem crossing* (ISC) (physical pathway)

$$^1O_2 + \text{carotenoid} \rightarrow {}^3O_2 + {}^3\text{carotenoid} \rightarrow {}^3O_2 + \text{carotenoid (+ heat)} \quad (1)$$

In contrast to physical quenching, there are also less efficient but concomitant processes involving real chemical reactions (chemical pathway).[10] For example, chemical oxidation reactions, which result in the destruction of carotenoids and thus in the loss of antioxidant protection (i.e. these are not *catalytic* processes), have been observed[11−13]

$$^1O_2 + \text{carotenoid} \rightarrow \text{chemical pathway} \quad (2)$$

The specific reactions involved in the chemical pathway (eq 2) are still not completely understood. It has been shown that the observed products arising from photosensitized carotenoid oxidation[11] seem to be accounted for by direct oxygen addition to the polyene rather than by free radical-mediated autoxidation (in photooxidation reactions, excited-state photosensitizers can

[†] Università di Bologna.

[‡] King's College.

(1) (a) Bensasson, R. V.; Land, E. J.; Truscott, T. G. *Excited States and Free Radicals in Biology and Medicine*; Oxford University Press: New York, 1993; pp 201−227. (b) Light-Harvesting Physics Workshop, Bristonas, Lithuania, September 1997; Special issue of the *J. Phys. Chem.* **1997**, *101*, 7197−7360.

(2) Blot, W. J.; li, J.-Y.; Taylor, P. R.; Guo, W.; Dawsey, S.; Wrang, G.-Q.; Yang, C. S.; Zheng, S.-F.; Gail, M.; Li, G.-Y.; Yu, Y.; Liu, B.-Q.; Tangrea, J.; Sun, Y.-H.; Liu, F.; Fraumeni, J. F., Jr.; Zhang, Y.-H.; Li, B. *J. Natl. Cancer Inst.* **1993**, *85*, 1483−1492.

(3) Burton, G. W.; Ingold, K. U. *Science* **1984**, *224*, 569.

(4) Everett, S. A.; Kundu, S. C.; Maddix, S.; Willson, R. L. *Biochem. Soc. Trans.* **1995**, *23*, 230.

(5) Ozhogina, O. A.; Kasaikina, O. T. *Free Radical Biol. Med.* **1995**, *19*, 575.

(6) Mathis, P. In *Organic Photochemistry and Photobiology*; Horspool, W. M., Song, P.-S., Eds.; CRC Press: New York, 1995; Chapter 16, p 1412.

(7) Ames, B. N. *Science* **1983**, *221*, 1256.

(8) (a) Tinkler, J. H.; Tavender, S. M.; Parker, A. W.; McGarvey, D. J.; Mulroy, L.; Truscott, T. G. *J. Am. Chem. Soc.* **1996**, *118*, 1756. (b) Bohm, F.; Edge, R.; Land, E. J.; McGarvey, D. J.; Truscott, T. G. *J. Am. Chem. Soc.* **1997**, *119*, 621−622.

(9) (a) Conn, P. F.; Schalch, W.; Truscott, T. G. *J. Photochem. Photobiol. B* **1991**, *11*, 41−47. (b) Speranza, G.; Manitto, P.; Monti, D. *J. Photochem. Photobiol. B* **1990**, *8*, 51−56.

(10) Foote, C. S. In *Singlet Oxygen*; Wasserman, H. H., Murray, R. W., Eds.; Academic Press: New York, 1979; pp 139−171.

(11) Stratton, S. P.; Schaefer W. H.; Liebler, D. *Chem. Res. Toxicol.* **1993**, *6*, 542.

(12) Schenck, G. O.; Schade, G. *Chimia* **1970**, *24*, 13.

(13) Hasegawa, K.; Macmillan, J. D.; Maxwell, W. A.; Chichester, C. O. *Photochem. Photobiol.* **1969**, *9*, 165−169.

S0002-7863(98)00527-7 CCC: $15.00 
Published on Web 09/22/1998

**Scheme 1**

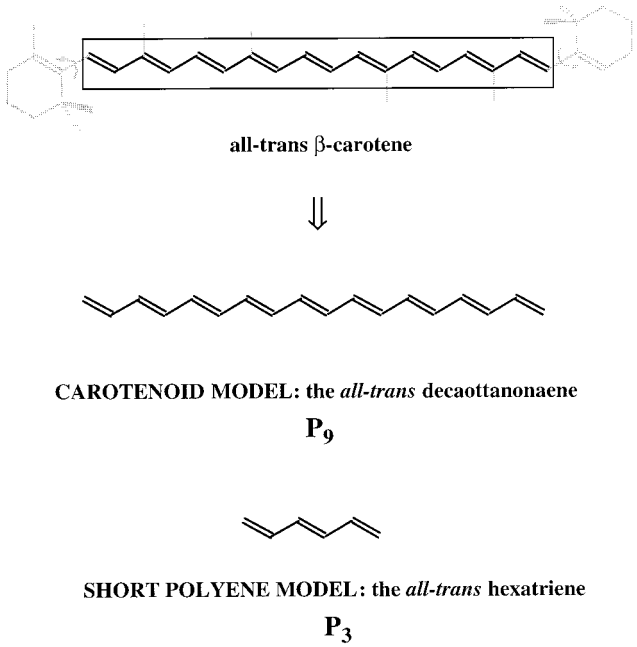


**Scheme 2**

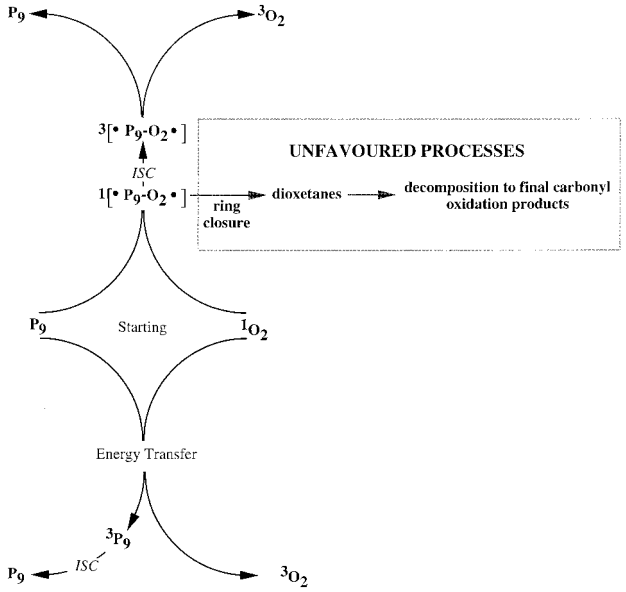


produce free radicals which, in principle, can oxidize carotenoids). However, it is not clear whether the observed oxidation products (which include apocarotenal chain cleavage fragments[11]) are formed by the direct addition of singlet-oxygen to the carotenoid system or by the reaction between the triplet-oxygen ($^3O_2$) and the triplet-carotenoid ($^3$carotenoid) produced by the main energy transfer process (eq 1). Moreover, other competing chemical reactions could be responsible for alternative *catalytic* singlet-oxygen quenching pathways. These processes, even if less efficient than energy transfer (eq 1), could be competitive with oxidation reactions.

The importance of the carotenoids/singlet-oxygen interaction in biology and the scientific interest focused upon these intriguing processes provide the motivation for the present theoretical study. A density functional theory (DFT) approach has been used to investigate the reactions involved in the attack of $^1O_2$ to the *all-trans*-decaottanonaene (**$P_9$**), a polyene with 9 conjugated double bonds, which has been chosen as the carotenoid model (see Scheme 1). The 9 conjugated double bond moiety is, in fact, a common feature in many carotenoids,[1,9a] while the substituents at the two ends of the chain may be different (see Figure 1). There are, in fact, several carotenoid systems with only 9 conjugated double bonds, such as violaxantin and neurosphorene, which show a singlet-oxygen quenching efficiency and a chemical reactivity comparable to that of $\beta$-carotene and longer carotenoids[9a] (Figure 1). In the carotenoid model **$P_9$**, all of the methyl substituents have been eliminated (see Scheme 1), thus neglecting the steric interactions between $^1O_2$ and the methyl groups.

As we shall presently discuss in detail, our theoretical study shows that, in addition to the main energy transfer pathway (eq 1) which is almost barrierless (Scheme 2 bottom), there are secondary (Scheme 2 top) but concomitant low energy barrier reactions (eq 2) leading to biradical intermediates via direct addition of $^1O_2$ to carbon−carbon double bonds of **$P_9$**. These biradicals may undergo ring closure to 1,2-addition dioxetane products whose subsequent decomposition leads to the final carbonyl chain cleavage oxidation fragments.[11−12] However these biradicals can also lead, through an $S_0 \rightarrow T_1$ ISC, to an alternative chemically mediated *catalytic* (**$P_9$** regeneration)

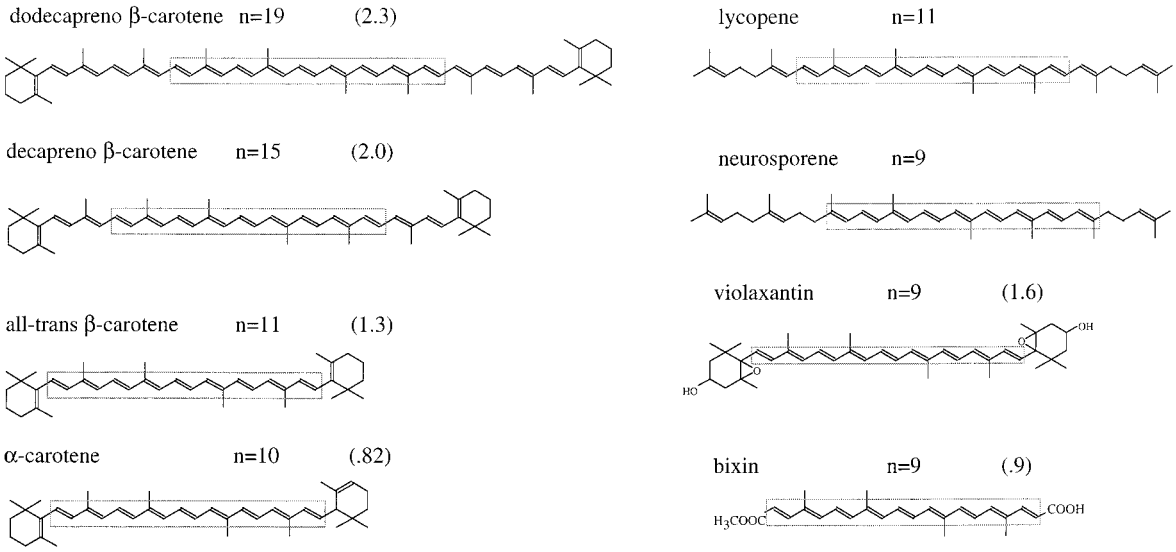


**Figure 1.** Typical carotenoid structures (where *n* is the number of conjugated C−C double bonds). The available second-order rate constants ($10^{10}$ $K_q$ $M^{-1}$ $s^{-1}$) for the quenching of singlet-oxygen are given in parentheses.[9a] The common 9 double bond moiety is given in frame.

quenching of singlet-oxygen which is returned to its triplet deactivated ground state through a dissociation process on $T_1$. This *catalytic* singlet-oxygen quenching pathway seems to be preferred (or at least competitive) with respect to oxidation reactions.

To assess the accuracy that can be obtained in a DFT study of the reaction between $^1O_2$ and a polyene, we have investigated a model reaction involving a shorter polyene system, the *all-trans*-hexatriene (**P₃** in Scheme 1). This model reaction has been investigated both at the DFT level and (for some energy values) at the multireference Møller−Plesset perturbation theory level (CAS-PT2).[14] The overall topology has been checked via analytical frequency calculations (see Computational Details and the Appendix).

## 2. Computational Details

All computations reported in this paper have been performed (unless otherwise specified) with DFT using a 6-31G* basis set and the unrestricted Becke3-LYP functional (UB3LYP).[15] The structures of all the critical points have been fully optimized using an analytical gradient procedure with the methods available in the Gaussian94 package of programs.[16b] Since the Becke3 exchange functional includes some Hartree−Fock exchange, it is appropriate to perform spin projection. Spin-projected energies have been calculated with the approximate spin-correction procedure proposed by Yamaguchi et al.,[17a] which has been recently applied by Houk et al.[17b] in the study of the two-step diradical mechanism of the Diels−Alder reaction of butadiene and ethylene. We have chosen this spin-correction procedure because it seems to provide reasonable energies for singlet-diradicals and therefore for species similar to those investigated in the present paper (for an application, see ref 17b). Recently it has been suggested[17c] that spin projection can degrade the quality of potential energy surfaces calculated by density functional methods. However, in the present case, comparison with experimental energies (when available) and with CAS-SCF and PT2 values (as described in detail in the Appendix) indicates that spin correction works satisfactorily.

In a previous paper[18] we have shown that ground-state isomerization barriers of long-chain conjugated polyenes may be adequately studied with a UB3LYP/6-31G* approach (with an error less than 1 kcal mol$^{-1}$). This is a first indication that the methods used here can be sufficiently accurate. To further "calibrate" the DFT/UB3LYP results, we could compare the DFT results with some structures investigated at the CAS-SCF and PT2 levels. However, the size of the **P₉** + $^1O_2$ system is too big to perform CAS-SCF[16a] and PT2[14a] computations. Thus, to calibrate the DFT/B3LYP results we have reoptimized some structures for the smaller system (**P₃** + $^1O_2$) at the CAS-SCF/6-31G* level (see the Appendix). For such computations we have used an active space involving 10 orbitals/12 electrons (the 6 $\pi$ orbitals/6 electrons of **P₃** + 4 $\pi$ orbitals/6 electrons of $O_2$). The energetics have then been refined via single-point computations at the multireference Møller−Plesset perturbation level of theory using the PT2F method included in MOLCAS-3[14b] (expanding the active space to 12 orbitals and 14 electrons). To compare DFT versus CAS-SCF $^1O_2$ optimized structures, we have reoptimized $^1O_2$ at the CAS-SCF/6-31G* level using the same 4 $\pi$ orbitals/6 electrons CAS. For the shorter system (**P₃** + $^1O_2$), we have also characterized (via DFT analytical frequency calculations) the nature of all the optimized stationary points, thus providing an indirect characterization of the corresponding points computed in the longer system (see the Appendix for a summary of the results on this shorter system). To assess the reliability of the hypothesis that peroxyl diradical minima may have a facile $S_0 \rightarrow T_1$ ISC, we have estimated the $S_0/T_1$ *spin−orbit coupling* via single-point CAS-SCF computations at the DFT/B3LYP diradical minimum structure optimized for the shorter system, using a 3 orbitals/4 electrons CAS (the two SOMO and a p-type oxygen lone pair) with Slater determinants and a 6-31G* basis set. Finally, DFT wave function stability checks have been performed, as will be explicitly stated in section 3.

## 3. *all-trans*-Decaottanonaene (P₉) + Singlet-Oxygen ($^1O_2$)

In this section we report the results obtained in the computational study of the reactions between $^1O_2$ and **P₉**. We have focused our study on the processes represented in Scheme 3.

There are four central processes which we shall discuss in the following subsections: (i) the energy transfer or physical quenching process plus ISC, (ii) the 1,2-addition of $^1O_2$, (iii) the diradical ISC plus triplet dissociation, and (iv) the triplet−triplet recombination. More chemical reactions have been documented in the literature involving carotenoid systems, e.g. the 1,4-addition of $^1O_2$ involving the $\beta$-ionone ring double bond as well as other more complex processes.[10−13] The effects of the substituents at the two ends of the chain are neglected in the model system, as well as the steric effect of the methyl groups. Since most of the observed chemical processes seems to involve oxygen addition to the polyenic chain bouble bonds,[11] we think that the studied reaction pattern (Scheme 3) is quite well representative and reliable for such kinds of mechanisms.

**(i) The Energy Transfer Process Plus ISC.** Carotenoids undergo a very efficient energy transfer process[1,9] in which oxygen is deactivated to its ground state ($^3O_2$), while the carotenoid system (**P₉** in our model reactions, see Scheme 3) is excited to its triplet state $T_1$. After relaxation, $T_1 \rightarrow S_0$ ISC regenerates carotene (with heat production) in its ground-state minimum (the initial reactant). Therefore, the overall process is a *catalytic* reaction with no consumption of carotene (eq 1).

**Energy Transfer.** Energy transfer rate is not only a matter of energetics, but it also depends on vibronic interactions, short distance interactions (such as overlap of the electron clouds), and long-range antenna-type dipole−dipole interactions, according to the type (short range or long range) of energy transfer

(14) (a) Andersson, K.; Malmqvist, P.-A.; Ross, B. O. *J. Chem. Phys.* **1992**, *96*, 1218. (b) *MOLCAS*, Version 3, Andersson, K.; Blomberg, M. R. A.; Fülscher, M.; Kellö, V.; Lindh, R.; Malmqvist, P.-A.; Noga, J.; Olsen, J.; Roos, B. O.; Sadlej, A. J.; Siegbahn, P. E. M.; Urban, M.; Widmark, P. O.; University of Lund, Sweden, 1994.

(15) Becke, A. D. *J. Chem. Phys.* **1993**, *98*, 1293.

(16) (a) Roos, B. O. *Adv. Chem. Phys.* **1987**, *69*, 399−446. (b) All of the optimizations at the MC-SCF and DFT(UB3LYP) levels (with a 6-31G* basis set) have been performed using the computational tools available in *Gaussian 94*, Revision B.2; Frisch, M. J.; Trucks, G. W.; Schlegel, H. B.; Gill, P. M. W.; Johnson, B. G.; Robb, M. A.; Cheeseman, J. R.; Keith, T.; Petersson, G. A.; Montgomery, J. A.; Raghavachari, K.; Al-Laham, M. A.; Zakrzewski, V. G.; Ortiz, J. V.; Foresman, J. B.; Peng, C. Y.; Ayala, P. Y.; Chen, W.; Wong, M. W.; Andres, J. L.; Replogle, E. S.; Gomperts, R.; Martin, R. L.; Fox, D. J.; Binkley, J. S.; Defrees, D. J.; Baker, J.; Stewart, J. P.; Head-Gordon, M.; Gonzalez, C.; Pople, J. A.; Gaussian, Inc., Pittsburgh, PA, 1995.

(17) (a) To evaluate the effect of spin projection on the singlet energy, we have computed the UB3LYP/6-31G* singlet ($^1E_{(UB)}$), triplet ($^3E_{(UB)}$), and singlet spin-corrected ($^1E_{(SC)}$) energies, applying the approximate spin-correction procedure proposed by Yamaguchi et al. (see Yamaguchi, K.; Jensen, F.; Dorigo, A.; Houk, K. N.; *Chem. Phys. Lett.* **1988**, *149*, 537 and Yamanaka, S.; Kawakami, T.; Nagao, H.; Yamaguchi, K. *Chem. Phys. Lett.* **1994**, *231*, 25) where it is assumed that singlet energy contamination arises only by the first higher multiplicity state, i.e. the $T_1$ state in our system

$$\Psi_{(UB)} = c_s{}^1\phi + c_T{}^3\phi$$

$$^1E_{(SC)} = {}^1E_{(UB)} + f_{SC}[{}^1E_{(UB)} - {}^3E_{(UB)}]$$

$$f_{SC} = \frac{c_T{}^2}{1 - c_s{}^2} \approx \frac{{}^1\langle S^2\rangle}{{}^3\langle S^2\rangle - {}^1\langle S^2\rangle}$$

(b) Goldstein, E.; Beno, B.; Houk, K. N. *J. Am. Chem. Soc.* **1996**, *118*, 6036−6043. (c) Wittbrodt, J. M.; Schlegel, M. B. *J. Chem. Phys.* **1996**, *105*, 6574.

(18) Bernardi, F.; Garavelli, M.; Olivucci, M.; Robb, M. A. *Mol. Phys.* **1997**, *92*, 359−364.

**Scheme 3**

**$O_2$ + $P_9$ REACTION PATTERN**

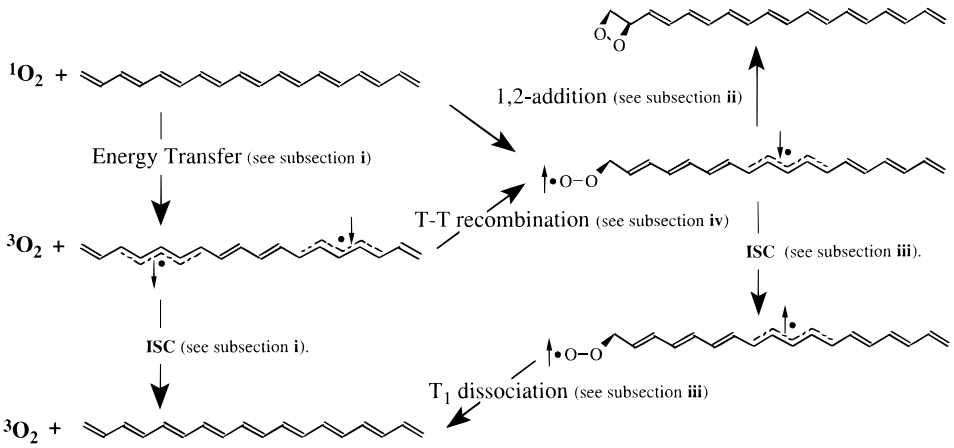


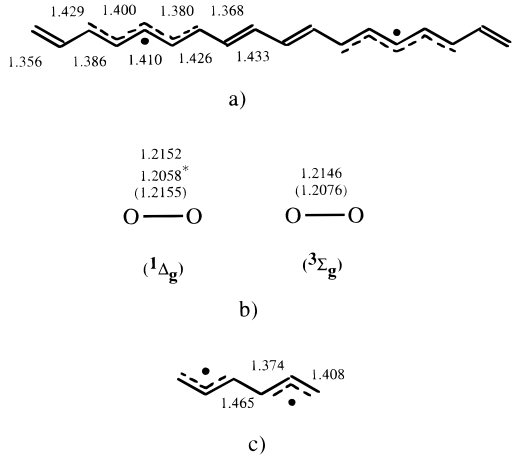


**Figure 2.** DFT optimized structures (quoted values in Å) for: (a) the relaxed *all-trans*-$\mathbf{P_9}$ $T_1$ minimum ($\mathbf{P_{9/Trip\text{-}Min}}$); (b) the singlet- and triplet-oxygen molecule (the starred value refers to CAS-SCF/6-31G* optimization, and the experimental values are given in parentheses); (c) the relaxed *all-trans*-$\mathbf{P_3}$ $T_1$ minimum ($\mathbf{P_{3/Trip\text{-}Min}}$).

involved.[19] However a very low-energy barrier is a prerequisite for a fast reaction of this type. Indeed, the experimental evidence for a process almost approaching the diffusion control limit suggests a similar energy level for triplet $\beta$-carotene and $^1O_2$[1] (which justifies an almost barrierless path).

Our DFT computational study provides information only on the energetics of a possible physical quenching path (eq 1), its energy profile, and its activation energy, without considering the other factors controlling the energy transfer. Such a study can give an indication of the energetic feasibility of the process, i.e. about the existence of an energetically favored route connecting the singlet−singlet ($^1\mathbf{P_9} + {}^1O_2$) starting reactants to the triplet−triplet ($^3\mathbf{P_9} + {}^3O_2$) products.

The carotenoid model $\mathbf{P_9}$ has many structural features of the previously studied[18] *all-trans* 11 double bond linear polyene ($\mathbf{P_{11}}$). The planar structure of the $\mathbf{P_9}$ *all-trans* $T_1$ minimum ($\mathbf{P_{9/Trip\text{-}Min}}$) is found to be 11.6 kcal mol$^{-1}$ more stable than the Franck−Condon (FC) $T_1$ structure. For the $T_1$ minimum, a bond order inversion-region (with respect to the $S_0$ optimized minimum $\mathbf{P_{9/Sing\text{-}Min}}$) is localized in the central part of the polyene. Thus, the $T_1$ minimum is a planar diradicaloid system

**Table 1.** B3LYP/6-31G* Relative Energies ($\Delta E$) and $\langle S^2\rangle$ Values for the *all-trans* Linear Polyenes ($\mathbf{P_{11}}$, $\mathbf{P_9}$, and $\mathbf{P_3}$) and Oxygen Molecule

| polyene | state | $\langle S^2\rangle$ | $\Delta E$ (kcal mol$^{-1}$)[a] |
|---|---|---|---|
| $\mathbf{P_{11/Sing\text{-}Min}}$[b] | ($S_0$) | 0.00 | 0.0[d] |
| | ($T_1$) | 2.08 | 26.1 |
| $\mathbf{P_{11/Trip\text{-}Min}}$[b] | ($S_0$) | 0.89 | 2.3 (7.4) |
| | ($T_1$) | 2.12 | 14.5 |
| $\mathbf{P_{9/Sing\text{-}Min}}$ | ($S_0$) | 0.00 | 0.0[e] |
| | ($T_1$) | 2.06 | 29.2 |
| $\mathbf{P_{9/Trip\text{-}Min}}$ | ($S_0$) | 0.73 | 3.8 (8.6) |
| | ($T_1$) | 2.10 | 17.6 |
| $\mathbf{P_{3/Sing\text{-}Min}}$ | ($S_0$) | 0.00 | 0.0[f] |
| | ($T_1$) | 2.02 | 58.7 |
| $\mathbf{P_{3/Trip\text{-}Min}}$ | ($S_0$) | .00 | 13.8 |
| | ($T_1$) | 2.03 | 44.3 |
| $^1O_2$[c] | ($^3\Sigma_g$) | 2.01 | 0.0[g] |
| | ($^1\Delta_g$) | 1.00 | 20.9 (10.4) |
| $^3O_2$[c] | ($^3\Sigma_g$) | 2.01 | 0.0[h] |
| | ($^1\Delta_g$) | 1.00 | 20.9 (10.4) |

[a] When spin-projection is applied (see Computational Details and ref 17), the spin-contaminated values are reported in parentheses. [b] $\mathbf{P_{11}}$ minima and energies have been reported in ref 18. [c] DFT optimized singlet- and triplet-oxygen are almost identical. [d] Absolute energy (au) −852.659 34. [e] Absolute energy (au) −697.843 78. [f] Absolute energy (au) −233.398 55. [g] Absolute energy (au) −150.320 04. [h] Absolute energy (au) −150.320 04.

which can be qualitatively described with the two unpaired electrons (inversion points) delocalized in the center of each symmetric half (Figure 2). The $S_0 \rightarrow T_1$ vertical excitation energy is 29.2 kcal mol$^{-1}$, somewhat higher than the 26.1 kcal mol$^{-1}$ computed for the longer $\mathbf{P_{11}}$ conjugated polyene[18] (see Table 1 for energy values). The UB3LYP method gives, for the optimized singlet-oxygen, an $\langle S^2\rangle$ expectation value of 1.0, i.e. an equal mixture of singlet and triplet. Spin correction[17a] leads to a triplet−singlet energy gap (Table 1) which is in good agreement with the available experimental energy difference[1] between the triplet and Δ-singlet states (20.9 kcal mol$^{-1}$ compared to 22.4 kcal mol$^{-1}$). Furthermore, the optimized O−O bond distance (Figure 2b) reproduces very well the experimental value[20] observed for the Δ-singlet state[21a] (1.2152 Å vs 1.2155 Å).

To determine a possible energy transfer path, we have performed a *linear interpolation* between two optimized elec-

(19) Gilbert, A.; Bargott, S. *Essentials of Molecular Photochemistry*; Blackwell Scientific Publications: Oxford, 1991; pp 167−181.

(20) Berry, R. S.; Rice, S. A.; Ross, J. *Physical Chemistry*; John Wiley & Sons: 1980; Vol. I, p 295.

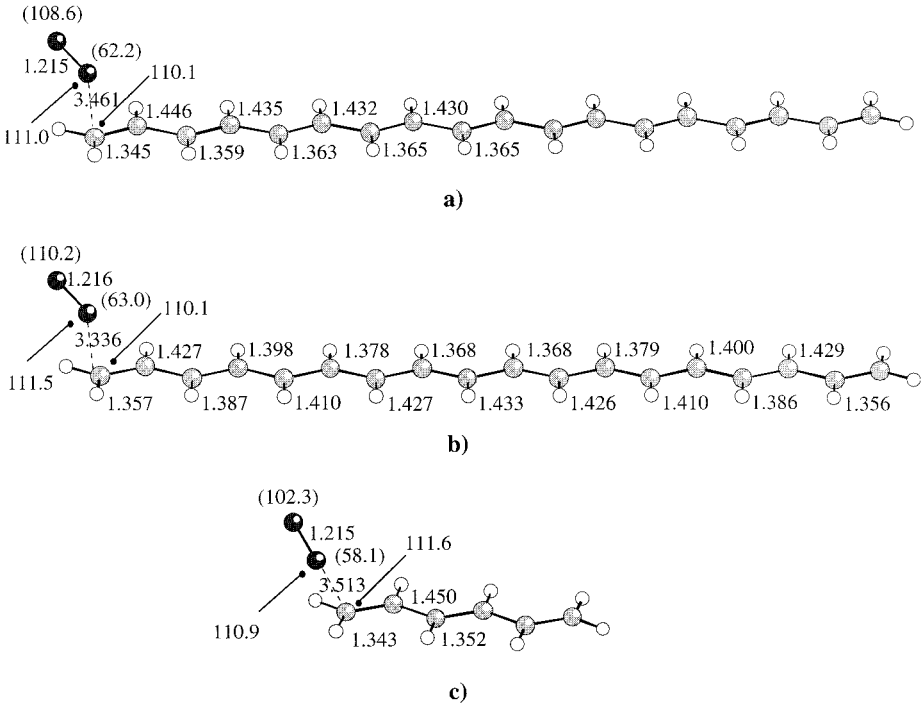


**Figure 3.** DFT optimized structures for: (a) the singlet−singlet [$^1O_2$···$^1$**P**$_{9\text{/Sing-Min}}$] complex; (b) the triplet−triplet [$^3O_2$···$^3$**P**$_{9\text{/Trip-Min}}$] complex; (c) the singlet−singlet [$^1O_2$···$^1$**P**$_{3\text{/Sing-Min}}$] complex. Bond lengths in Å; angles and dihedral angles (OOC/OCC and OCC/CCC are given in parentheses) in degrees.

trostatic complexes, the singlet−singlet complex [$^1O_2$···$^1$**P**$_{9\text{/Sing-Min}}$], which represents the starting reactant, and the relaxed triplet−triplet complex [$^3O_2$···$^3$**P**$_{9\text{/Trip-Min}}$], which represents the final product (Figure 3a, b). Single-point energy calculations have then been performed along the interpolated path[21b] (10 steps have been chosen). The initial position of the oxygen molecule in the two electrostatic complexes has been arbitrarily chosen to be near the external double bond (which seems to be the most reactive position for $^1O_2$ attack, see subsection **ii**). The linear interpolation between the two complexes describes the changes occurring in the polyene moiety when energy transfer takes place, going from the singlet relaxed structure ($^1$**P**$_{9\text{/Sing-Min}}$) to the triplet relaxed structure ($^3$**P**$_{9\text{/Trip-Min}}$) (mainly associated with the inversion of the bond order in the center of the polyene, as stated above). The relaxed structures of $^1O_2$ and $^3O_2$ remain almost identical in this interpolation. Spin-projection on the singlet−singlet [$^1O_2$···$^1$**P**$_{9\text{/Sing-Min}}$] wave function is required[21c] to obtain a correct energy profile but for the triplet−triplet coupling (globally again a singlet state wave function), no decontamination is needed.[22a] Due to the abrupt change in the singlet state wave function passing from a singlet−singlet coupling ($^1$**P**$_9$ + $^1O_2$) to a triplet−triplet coupling ($^3$**P**$_9$ + $^3O_2$) description, it was possible to follow each coupling situation all along the linear interpolation. In this way we have determined the *diabatic* components of the path as well as the singlet ground-state and the singlet excited-state surfaces along the linear interpolated cross section.[22b] The stability of the DFT wave function in the two complexes (the reactant and the product) has been checked both in the singlet−singlet and triplet−triplet coupling situations (see Table 2 for energy values and Figure 4 for the energy profiles).

Our results suggest that the energy transfer process (physical quenching) is energetically very favored, being associated with an almost barrierless pathway, even in the case of a simple linear interpolation (which must be an upper boundary to the energy). Along the linear interpolation path, going from a singlet−singlet

**Table 2.** B3LYP/6-31G* Relative Energies ($\Delta E$) and $\langle S^2\rangle$ Values for the Stationary Points of the **P**$_9$ Plus Oxygen System

| structures | state | $\langle S^2\rangle$ | $\Delta E^a$ |
|---|---|---|---|
| **S**−**S** complex | $(T_1)^b$ | 2.01 | 0.0[e] |
| $O_2$···**P**$_{9\text{/Sing-Min}}$ | $(S_0)^c$ | 1.00 | 20.6 (10.3) |
| | $(S^*)^d$ | 2.04 | 29.4 |
| **T**−**T** complex | $(S_0)^d$ | 2.09 | 17.4 |
| $O_2$···**P**$_{9\text{/Trip-Min}}$ | $(S^*)^c$ | 1.73 | 24.3[f] (18.6) |
| **TS**$_1$ | $(T_1)$ | 2.29 | 13.3 |
| | $(S_0)$ | 1.24 | 25.3 (18.8) |
| **TS**$_{1\text{-central}}$ | $(T_1)$ | 2.19 | 20.0 |
| | $(S_0)$ | 1.08 | 25.9 (23.0) |
| diradical-minimum | $(S_0)$ | 1.15 | 4.7 (5.0) |
| | $(T_1)$ | 2.15 | 5.3 |
| **TS**$_2$ | $(S_0)$ | 0.77 | 18.9 (23.3) |
| | $(T_1)$ | 2.12 | 30.9 |
| **TS**$_3$ | $(T_1)$ | 2.28 | 14.1 |
| **TS**$_4$ | $(T_1)$ | 2.57 | 15.6 |
| | $(S_0)$ | 1.51 | 30.8 (21.8) |
| dioxetane minimum | $(S_0)$ | 0.00 | −4.5 |

[a] When spin-projection is applied (see Computational Details and ref 17), the spin-contaminated values are reported in parentheses. [b] The triplet overall wave function refers to a triplet-oxygen plus singlet−polyene coupling. [c] The singlet overall wave function refers to a singlet-oxygen plus singlet−polyene coupling. [d] The singlet overall wave function refers to a triplet-oxygen plus triplet−polyene coupling. [e] Absolute energy (au) −848.163 98. [f] Spin-projection is applied to the energies computed for the two isolated fragments (see Table 1).

(21) (a) It is known that the $\Delta$ state of singlet-oxygen is given by two degenerate components, a closed shell component and an open shell one (called respectively $x^2 - y^2$ and $xy$), while the higher energy $\Sigma$ singlet-state is a closed shell (called $x^2 + y^2$). Since unrestricted-B3LYP converges on open-shell ($xy$) configuration, mixing with the closed-shell type $\Sigma$ state cannot occur. (b) We are confident that the energies of the complexes as well as those of the interpolated points (both in the singlet−singlet and triplet−triplet description) are correct because they are just a little lower (<1 kcal mol$^{-1}$ due to stabilization by electrostatic interactions) than the sum of the singly computed energies for the two isolated fragments in both coupling situations. (c) The resulting spin-projected values are obtained by summing either the decontaminated energies of the two isolated molecules or by direct decontamination of the electrostatic cluster energies; this has been done for the first points of the linear path from the reactants and leads to the same values apart from the <1 kcal mol$^{-1}$ cluster stabilization energy.

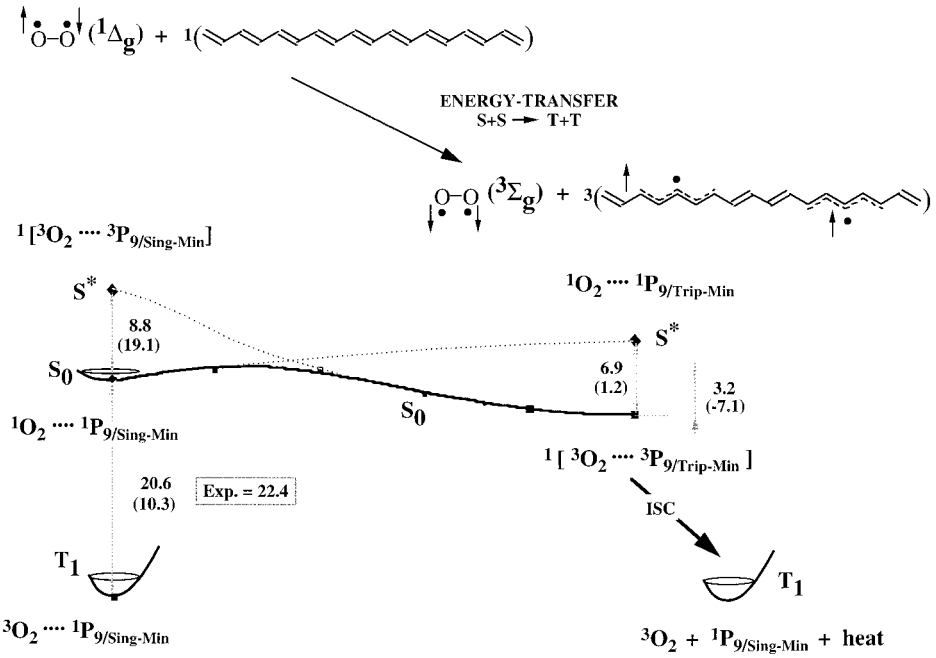


**Figure 4.** Linear interpolated DFT energy profile (values in kcal mol$^{-1}$) for the energy transfer process (see subsection **i**). Values in parentheses are spin-unprojected energies, while the experimental triplet−singlet energy gap[1] is given in the frame. Dotted lines represent the diabatic (singlet−singlet and triplet−triplet coupling) components of the energy transfer path. The relative positions for the triplet (**$T_1$**), singlet (**$S_0$**), and excited singlet (**S***) states of reactants and products are shown.

to a triplet−triplet coupling, a change in the spin densities of the system occurs. Of course, our linear interpolation is only one of the infinite ways one can connect reactants with products. However, the fact that we have obtained an almost zero-energy barrier is a demonstration of the efficiency of such a process (at least from an energetic point of view). This result is consistent with the observation of a very fast process (most singlet-oxygen quenching rate constants for carotenoids have an order of magnitude of $10^{10}$ $M^{-1}$ $s^{-1}$,[1,9a] see Figure 1). Moreover, if we consider longer polyenes, where the $S_0 \rightarrow T_1$ vertical excitation energy is smaller (see the energy values in Table 1 for the 3, 9, and 11 double-bond polyenes), we should expect an even easier process because the crossing between the two *diabatic* surfaces should occur closer to the singlet−singlet reactant, due to a smaller energy gap between the ground- and excited-state singlets. (Long-chain carotenoids such as dodecapreno $\beta$-carotene (19 double bonds) or decapreno $\beta$-carotene (15 double bonds) have higher singlet-oxygen quenching rate constants than short-chain carotenoids such as violaxantin (9 double bonds),[9a] see Figure 1.)

**ISC Mechanism.** After energy transfer, a $T_1 \rightarrow S_0$ ISC will regenerate the carotene in the ground state. We have previously studied[18] an 11 double-bond polyene (with the same number of double bonds as $\beta$-carotene), and we have found a $T_1$ isomerization pathway connecting the planar *all-trans* to the central bond *cis* isomer (Figure 5). In the transition structure, the $T_1$ and $S_0$ states are degenerate. If we suppose that the ISC occurs near this point (where the singlet−triplet energy gap becomes very small) and thus we calculate the *all-trans* $T_1$ lifetime from the energy barrier (11 kcal mol$^{-1}$), considering a standard unimolecular preexponential factor of $10^{13}$ $s^{-1}$,[23] we estimate a value of 6 $\mu$s.[24] The observed lifetime for the *all-trans*-$\beta$-carotene $T_1$ state is about 5 $\mu$s[25] (in isolated conditions, without any heavy atom effect reducing the triplet lifetime) giving a surprising agreement with the computed value. Further, it is well-known that the triplet states of carotenoids are quenched by ground-state oxygen ($^3O_2$)[1,19,26]. This process is not an energy transfer but simply an enhanced ISC associated with the triplet-state character of the ground-state oxygen in the reaction complex with the carotenoid:

$$^3\mathrm{Car} + {}^3\mathrm{O_2} \rightarrow [{}^3\mathrm{Car}\cdots{}^3\mathrm{O_2}] \rightarrow \mathrm{Car} + {}^3\mathrm{O_2}$$

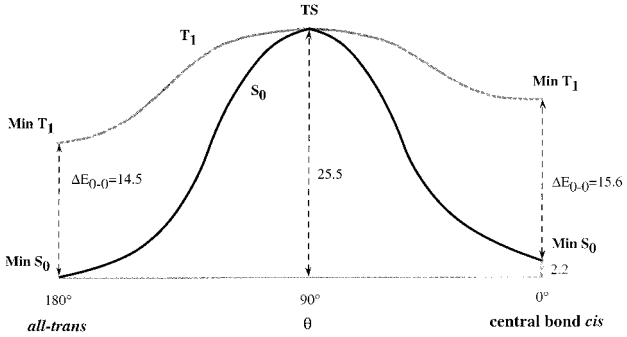


**Figure 5.** Simplified DFT singlet (**$S_0$**) and triplet (**$T_1$**) energy profiles for the isomerization about the central C−C bond of the $\beta$-carotene model **$P_{11}$**;[18] $\theta$ is the dihedral angle of rotation about the central double bond. **MIN S0**, **MIN T1** represent the $S_0$ and $T_1$ DFT optimized (*all-trans* or cis) minima connected by the transition state **TS**, respectively (see ref 18 for further details).

(22) (a) Actually, the computed energy values along the path are equal (again apart from the <1 kcal mol$^{-1}$ stabilization energy) to the sum of the energies computed for the two isolated fragments which have no spin-contamination, both triplet states having a correct $\langle S^2 \rangle$ value of 2 (see Table 1). (b) The *diabatic* components of the *adiabatic* electronic eigenfunctions describe the energy of a particular spin-coupling (see Olivucci, M., Ph.D. Thesis, University of Bologna, 1988), while the *adiabatic* functions represent the surfaces of the real states (the singlet ground and excited states in this case).

(23) Benson, S. W.; *Thermochemical Kinetics*; Wiley: New York, 1976.

(24) The rate constant is estimated using the simple Arrenius equation ($k = A\ e^{-E_a/RT}$, where $A$ is the preexponential factor) at the physiological temperature of 310 K. For unimolecular reactions the lifetime ($\tau$) is calculated as the inverse of the first-order rate constant ($\tau = k^{-1}$).

(25) Hashimoto, H.; Koyama, Y.; Ichimura, K.; Kobayashi, T. *Chem. Phys. Lett.* **1989**, *162*, 517.

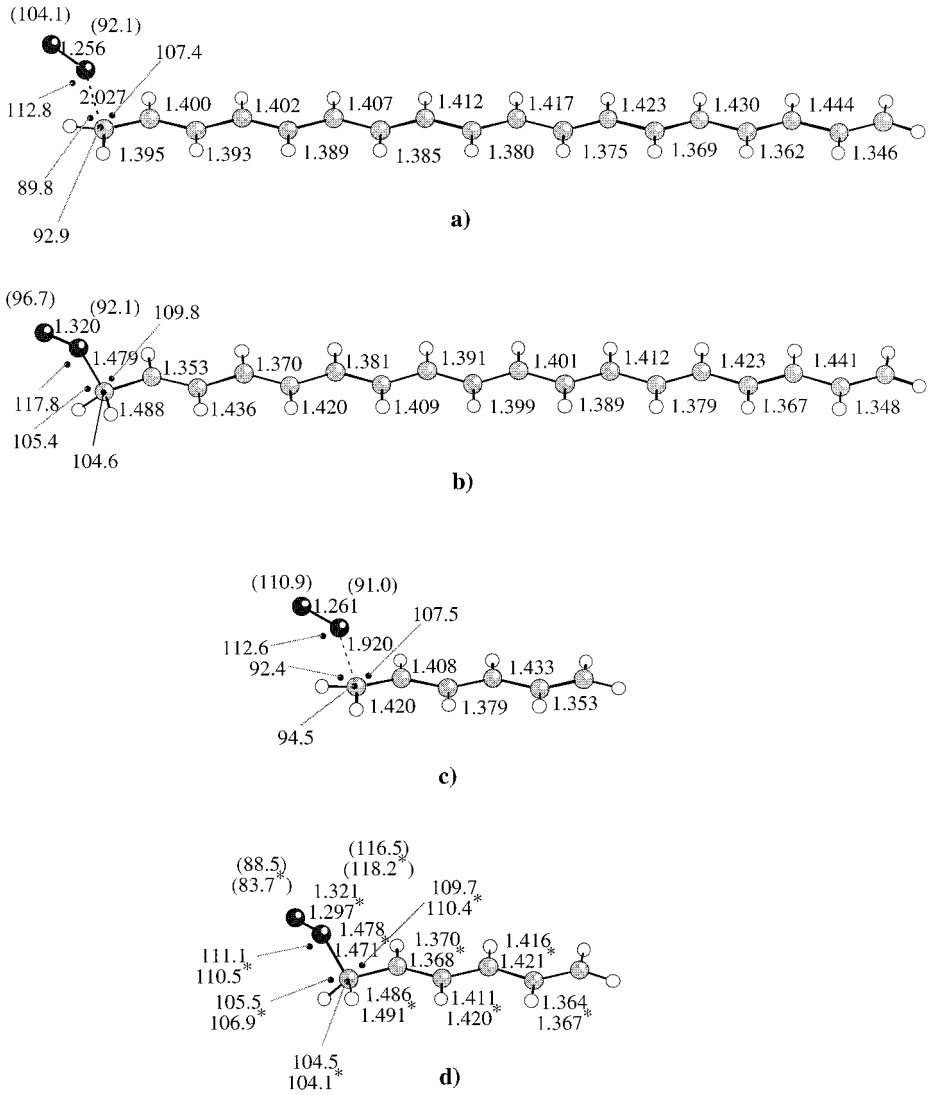


**Figure 6.** DFT optimized structures for: (a) the gauche transition state $\mathbf{TS_1}$; (b) the singlet (or triplet) diradical minimum [$\bullet\mathbf{P_9}-0_2\bullet$]; (c) the gauche transition state $\mathbf{TS_1}'$; and (d) the singlet (or triplet) diradical minimum [$\bullet\mathbf{P_3}-0_2\bullet$]. Starred values refer to CAS-SCF/6-31G* optimization. Bond lengths in Å; angles and dihedral angles (OOC/OCC and OCC/CCC are given in parentheses) in degrees.

Thus, in the presence of $^3O_2$, the triplet lifetime of carotene should be approximately reduced by 2 orders of magnitude (this is in general a good approximation[26]) and a ~10-ns triplet lifetime time scale is expected.

**(ii) 1,2-Addition of $^1O_2$.** Real chemical oxidation reactions have been observed[10−13] together with the dominant energy transfer process just discussed. The oxidation reactions result in the loss of carotenoids and antioxidant protection producing carbonyl chain cleavage oxidation fragments. The starting process is the direct singlet-oxygen attack upon the double bonds of the carotenoid model. We have studied this process to document the efficiency of such reactions as well as the relative reactivity, toward oxygen addition, of the different double bonds along the chain.

In ref 27, we have investigated the potential energy surface associated with the cycloaddition between $^1O_2$ and ethylene (but not the full surface including both the cycloaddition and ene reactions). In the case of cycloaddition, we have found that this reaction is not a pericyclic one-step concerted reaction but a two-step reaction which proceeds through a gauche attack with the formation of a singlet-diradical intermediate. This computational result suggests the investigation of a diradical approach, which is even more likely here (with a long polyene) due to a resonance-stabilization effect of the polyenic chain, favoring eventual diradical intermediates. Consequently, we have initially searched for a diradical transition state involving the $\mathbf{P_9}$ external double bond (the carotenoid model $\mathbf{P_9}$ has an *all-trans* configuration which allows 1,2-addition but excludes 1,4-cycloadditions and related transition states). A transition state ($\mathbf{TS_1}$, see Figure 6a) similar to the gauche transition state for the shorter ethylene case has been optimized. This critical point (with a low-energy barrier of 4.7 kcal mol$^{-1}$) leads to a singlet-diradical intermediate (see Figure 7 for the energy profiles) whose optimized structure is shown in Figure 6b (it is 15.9 kcal mol$^{-1}$ more stable than the reactants). We may view this biradical as composed of a peroxyl radical and of a resonance-stabilized *all-trans*-decaeptaottaenylic radical. Due to the extensive delocalization of the polyene radical, the reaction is easier (and the activation energy lower) with the long chain polyene than with short polyenes (see ethylene[27] and hexatriene in the Appendix) because the diradicaloid transition state is

(26) (a) McGlynn, S. P.; Azumi, T.; Kinoshita, M. *Molecular Spectroscopy of the Triplet State*; Prentice-Hall: Englewood Cliffs, NJ, 1969; pp 284−328. (b) Porter, G.; Sticf, L. J. *Nature* **1962**, *195*, 991.

(27) (a) Tonachini, G.; Schlegel, H. B.; Bernardi, F.; Robb, A. M. *J. Am. Chem. Soc.* **1990**, *112*, 483−491. (b) Tonachini, G.; Ghigo, G., personal communication.

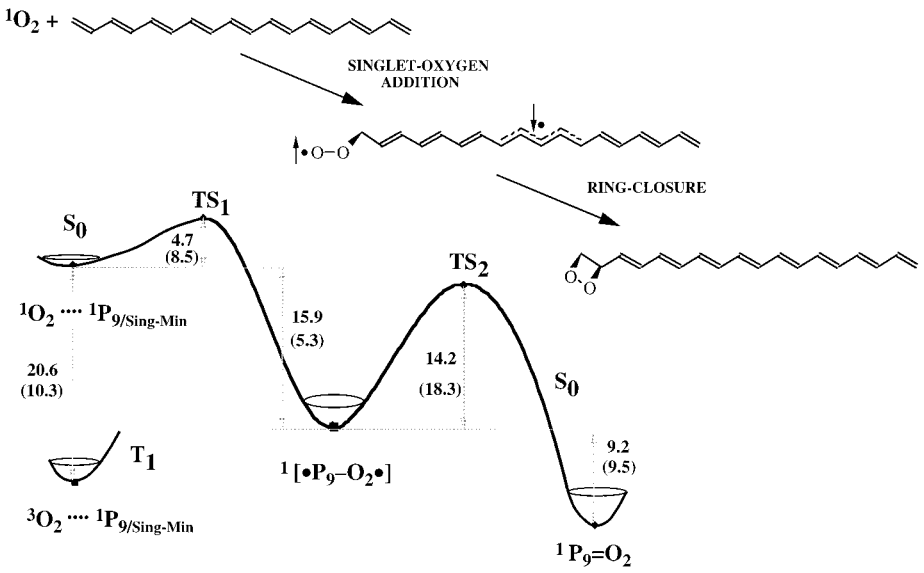


**Figure 7.** DFT energy profile (values in kcal mol$^{-1}$) for the 1,2-addition process: singlet-oxygen addition plus ring closure (see subsection **ii**). Values in parentheses represent spin-unprojected energies. The relative positions for the triplet ($\mathbf{T_1}$) and singlet ($\mathbf{S_0}$) states of the reactant, diradical intermediate, dioxetane product, and transition structures ($\mathbf{TS_1}$ and $\mathbf{TS_2}$) are shown.

stabilized (and the diradical product as well) by the resonance effect in the polyene fragment. Thus, in addition to demonstrating the main energy transfer pathway (eq 1), we have also demonstrated the existence of secondary low-energy barrier reactions leading to biradical intermediates via the direct addition of $^1O_2$ to the carbon−carbon double bonds of $\mathbf{P_9}$.

To test the reactivity of the different double bonds along the chain, we have optimized a similar transition state ($\mathbf{TS_{1\text{-}central}}$) for the attack to the central double bond. The energy barrier is somewhat higher (5.3 kcal mol$^{-1}$) due to a shorter polyene chain over which to delocalize the unpaired electron. We then expect that the activation energy will increase, going from the external to the most internal double bonds. However, the differences in the barriers are small, showing a similar resonance stabilization energy going from the decaeptaottaenylic to the nonatetraenylic fragment which is produced by the most inner double-bond attack. Thus, even if the external double bond seems to be the most reactive to a singlet-oxygen attack (and in fact it is the most exposed), we cannot exclude additions to other double bonds, and indeed, oxidation products produced by these reactions have been observed.[11]

After singlet-biradical formation, ring-closure reactions may occur on $S_0$ to form 1,2-addition dioxetane products through the recoupling of the two unpaired electrons. In the ethylene + $^1O_2$ example,[27a,b] this reaction has a small barrier (we computed a barrier of about 7 kcal mol$^{-1}$ with the 8 electrons/6 orbitals CAS and a 6-31G* basis set), arising mainly from the ring-strain contribution (produced in a 4-atom ring) which has to be overcome before a stabilization contribution, arising by the new forming C−O bond, becomes significant. In this simple system, the ring-strain contribution is probably the only destabilizing effect because recoupling reactions between radicals (as between a peroxyl and a primary radical) are known to be barrierless (or almost so).[28] This is not the case for our model system where the peroxyl radical reacts with an almost coupled adjacent double bond and a new "double bond breaking" contribution to the activation energy has to be added. These effects are responsible for the higher (14.2 kcal mol$^{-1}$) activation energy value we have computed at the optimized ring-closure transition state ($\mathbf{TS_2}$) (Figure 8a). In addition, the energy level of the optimized dioxetane product (Figure 8b) is 9.2 kcal mol$^{-1}$ below the diradical energy level (Figure 7 shows the reaction profiles, while all the energy values are summarized in Table 2).

Dioxetanes are quite unstable, and their decomposition will yield carbonyl products.[12] Carbonyl (apocarotenals) chain cleavage fragments have indeed been observed as singlet-oxygen oxidation products of $\beta$-carotene in experiments where they are accumulated over a long irradiation time.[11] In particular, the ones corresponding to external double bond breaking are the primary products, in agreement with the above-discussed higher reactivity of external double bonds.

**(iii) Triplet Dissociation.** At the diradical minimum structure, the $S_0$ and $T_1$ states are almost degenerate, and the optimized triplet-diradical minimum is virtually identical to the singlet one (Figure 6b) because the two unpaired electrons are so far away from each other that they do not interact. Therefore, the shape of the $S_0$ and $T_1$ potential energy surfaces are very similar because the interaction between the unpaired electrons remains small. The fact that the two (singlet and triplet) minima are almost identical and degenerate suggests the mechanistic hypothesis of an easy $S_0 \rightarrow T_1$ ISC involving the diradical intermediates. To test the reliability of this hypothesis, we have performed approximate *spin−orbit coupling* calculations (at the CAS-SCF level) on a similar shorter model system (hexatriene + $^1O_2$, see the Appendix and Computational Details). The magnitude of the computed approximate *spin−orbit coupling* is about 5 cm$^{-1}$, which is significant despite the long distance (even in the shorter model case) between the orbitals occupied by the two unpaired electrons (the two SOMO). Using the energy barrier of the dioxetane product (14.2 kcal mol$^{-1}$) and a standard unimolecular preexponential factor of $10^{13}$ s$^{-1}$,[23] we have estimated the singlet-diradical lifetime to be in the milliseconds (ms) time scale.[24] However, ISC rates in biradicals are well-known to be much shorter than milliseconds (they are at most in the microsecond ($\mu$s) range).[29] Therefore, we can assume that the ISC between the two states is operative and preferred (or at least competitive) with respect to the singlet ring-closure reaction as well as to the C−O bond-breaking

(28) Howard, J. A. *Free Radicals*; Kochi, J. L., Ed.; Wiley: New York, 1973; Vol. 2, pp 4−62.

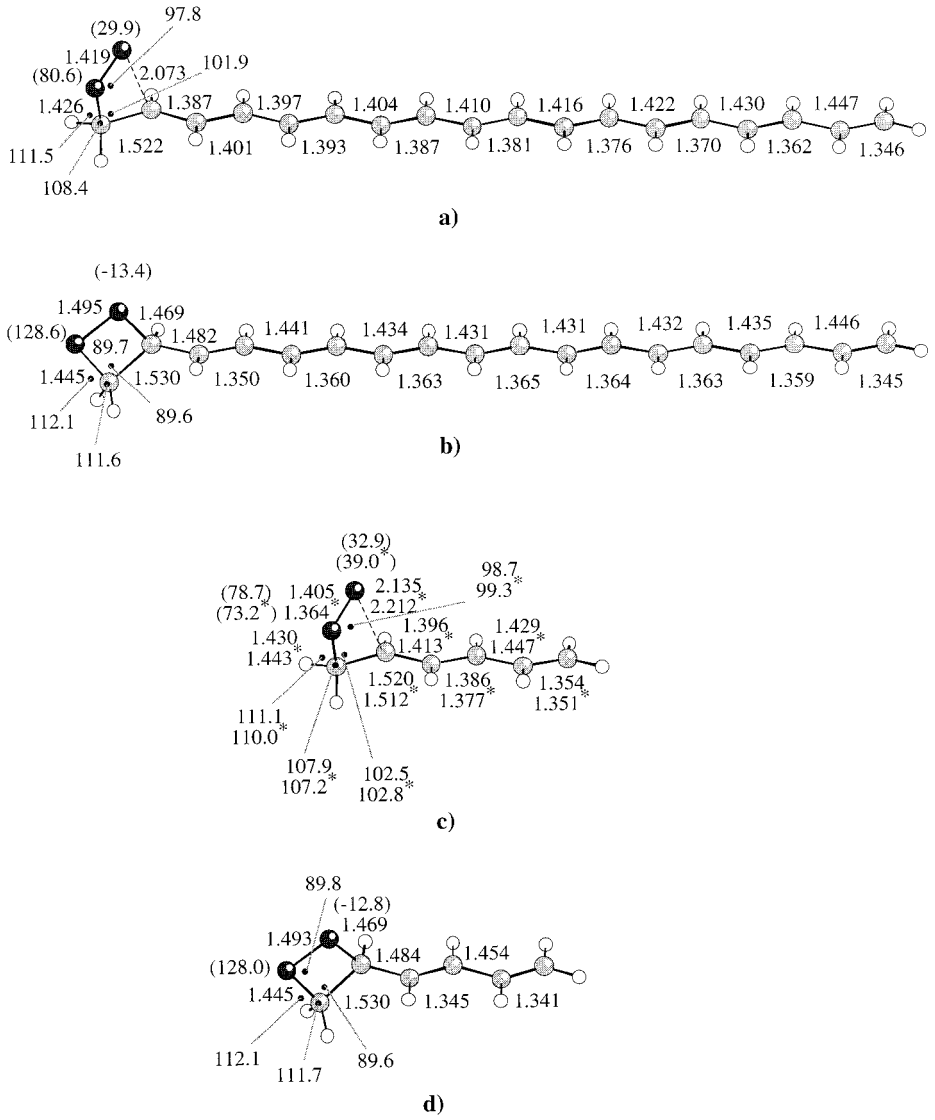


**Figure 8.** DFT optimized structures for: (a) the transition state $\mathbf{TS_2}$; (b) the dioxetane product $^1\mathbf{P_9}{=}0_2$; (c) the transition state $\mathbf{TS_2}'$; (d) the dioxetane product $^1\mathbf{P_3}{=}0_2$. Starred values refer to CAS-SCF/6-31G* optimization. Bond lengths in Å; angles and dihedral angles (OOC/OCC and OCC/CCC are given in parentheses) in degrees.

reaction back to the reactants (which is even more energetically demanding, see Figure 7).

After $S_0 \rightarrow T_1$ ISC has occurred, the system can undergo a C−O bond-breaking dissociation reaction on the $T_1$ state and the optimized transition structure $\mathbf{TS_3}$ (Figure 9a and Figure 10) has only a low 8.8 kcal mol$^{-1}$ activation energy. Due to the low $T_1$ dissociation barrier (we have estimated[24] the triplet-diradical lifetime to be in the 0.1 $\mu$s time scale), this bond-breaking reaction appears to be competitive with respect to oxidation reactions on the singlet state, leading to 1,2-addition dioxetane intermediates and then to final carbonyl products (see subsection **ii**). Further, the triplet dissociation bond-breaking process should be entropically more favorable than the singlet ring-closure reaction,[30] favoring the dissociation process and resulting in a smaller triplet diradical lifetime. Moreover, the computed barrier for the $^3O_2$ addition to the $\mathbf{P_9}$ model (14.1 kcal mol$^{-1}$) agrees very well with that estimated by a recent kinetic study[31] which leads to a value of 16 ± 1 kcal mol$^{-1}$ (see energies in Table 2).

(29) See Johnston, L. J.; Scaiano, J. C. *Chem. Rev.* **1989**, *89*, 521 for a collection of biradical lifetimes; note that none is longer than some microseconds. In particular, in the case of singlet−triplet degenerate diradicals, ISC may be induced by the *hyperfine coupling* (HFC) mechanism, thus reducing the lifetimes of the diradicals (the HFC can be probed by magnetic field effects and deuterium exchange experiments, see Wang, J.; Doubleday, C., Jr.; Turro, N. J. *J. Phys. Chem.* **1989**, *89*, 4780); in fact, HFC-induced ISC becomes operative whenever the singlet−triplet gap is almost zero (i.e. singlet and triplet are more or less degenerate) which is usually the case for all remote long-chain biradicals (with two weakly interacting uncoupled electrons) as it is for the studied situation (for more details, see Caldwell, R. A. in *Kinetics and Spectroscopy of Carbenes and Biradicals*, Platz, M., Ed.; Plenum Publishing: New York, 1990; pp 77).

(30) This trend has been verified for the shorter system (which is discussed in Appendix) by DFT analytical frequency calculations on the ring-closure transition state $\mathbf{TS_2}'$ (Figure 8c), the dissociation transition state $\mathbf{TS_3}'$ (Figure 9b) and the common diradical minimum (Figure 6d), obtaining respectively values of 90.2, 97.8, and 94.1 (cal mol$^{-1}$ K$^{-1}$) for the entropy and 78.5, 77.5, and 78.7 (kcal mol$^{-1}$) for the zero-point energies. Therefore, the zero-point energies also show the same trend, favoring the dissociation process and resulting in a smaller triplet-diradical lifetime. Moreover, the reversibility of oxygen−polyene addition (C−O bond cleavage with $^3O_2$ back production) is a well-known and well-studied process in peroxyl radical chemistry (see Porter, N. A.; Lehman, L. S.; Weber, B. A.; Smith, K. J. *J. Am. Chem. Soc.* **1981**, *103*, 6447; Porter, N. A.; Weber, B. A.; Weenen, H.; Kahn, J. A. *J. Am. Chem. Soc.* **1980**, *102*; 5597; Chan, H. W.-S.; Levett, G.; Matthew, J. A. *J. Chem. Soc., Chem. Commun.* **1978**, 756; Chan et al. *Chem. Phys. Lipids* **1979**, *24*, 245) where unstable polyenylic radicals are produced by the inverse endothermic reaction; thus, we expect that the computed exothermic triplet-diradical dissociation process is much more favored, producing the stable *closed shell* ground state of $\mathbf{P_9}$.

(31) Ej-Oualja, H.; Perrin, D.; Martin, R. *New J. Chem.* **1995**, *19*, 863.

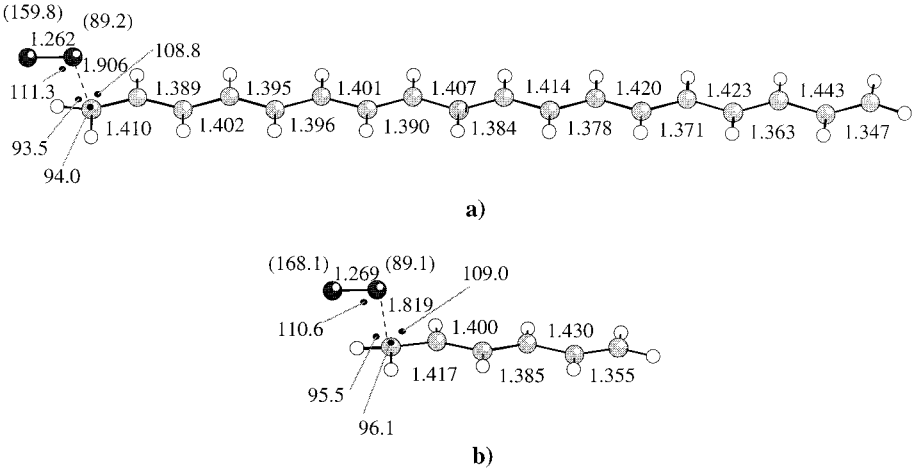


**Figure 9.** DFT optimized structures for: (a) the transition state $\mathbf{TS_3}$; (b) the transition state $\mathbf{TS_3'}$. Bond lengths in Å; angles and dihedral angles (OOC/OCC and OCC/CCC are given in parentheses) in degrees.

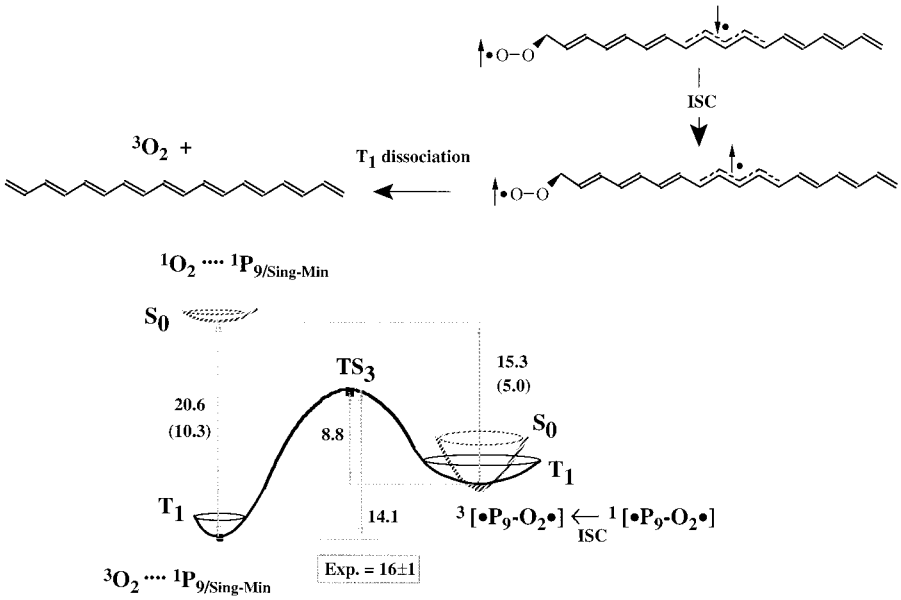


**Figure 10.** DFT energy profile (values in kcal mol$^{-1}$) for the $T_1$ dissociation process (see subsection **iii**). Values in parentheses represent spin-unprojected energies and the experimental[31] energy barrier is given in the frame. The relative positions for the triplet ($\mathbf{T_1}$) and singlet ($\mathbf{S_0}$) states of the diradical reactant, transition state ($\mathbf{TS_3}$), and final products are shown.

The dissociation reaction on $T_1$ produces oxygen in its triplet ground state and the $\mathbf{P_9}$ carotenoid model in its singlet relaxed ground state (Figure 10). These are the same final products of the energy transfer reaction followed by ISC (see Figure 4). Therefore, the overall process (singlet-diradical formation and ISC followed by triplet dissociation) provides an alternative chemically mediated *catalytic* quenching of singlet-oxygen which seems to be more favored than oxidation reactions.

The *catalytic* physical and chemical quenching of singlet-oxygen may act together in the observed carotenoid protection[1−8] of biological tissues against cellular damage by oxidation reactions. Oxidations, resulting in the loss of carotene and thus of antioxidant protection, could be favored much less than it can be expected initially, considering only the energy transfer processes. Carotenoid regeneration can, in fact, occur also through a competitive chemical singlet-oxygen quenching path.

**(iv) Triplet−Triplet Recombination.** The computed singlet-diradical minima can in principle be formed also by triplet−triplet recombination reactions (with C−O bond formation) involving the two triplet moieties ($^3O_2$ and $^3\mathbf{P_9}$) produced during the physical quenching pathway (energy transfer). The two triplets $^3O_2$ and $^3\mathbf{P_9}$ can be seen as two possibly interacting biradicals (see the reaction pattern in Scheme 3). To assess the reliability of this hypothesis, we have looked for a possible recombination reaction on $S_0$ (since the wave function has an overall singlet multiplicity) connecting the two molecules to the optimized diradical minimum. A transition state ($\mathbf{TS_4}$) describing this process (with an incipient C−O bond between the two triplet fragments, see Figure 11) has been localized (and DFT wave function stability has been checked) with a spin-projected (spin-contaminated) 13.4 (4.4) kcal mol$^{-1}$ energy barrier (Figure 12 and Table 2).

Recombination reactions are certainly not entropically favored, due to the loss of translational and rotational degrees of freedom. Thus, for this process we have supposed a bimolecular preexponential factor of $10^9$ M$^{-1}$ s$^{-1}$.[32] Even if we consider the lower 4.4 kcal mol$^{-1}$ (spin-contaminated) energy barrier, we obtain a $^3\mathbf{P_9}$ lifetime in the ms time scale,[33] while $\mathbf{P_9}$ $T_1 \rightarrow S_0$ ISC, in the presence of $^3O_2$, has been estimated in the 10-ns

(32) This is the rate constant for addition reactions between $^3O_2$ and resonance-stabilized alkyl radicals (see Hasegawa, K.; Patterson, L. K. *Photochem. Photobiol.* **1978**, *28*, 817−823) as $^3\mathbf{P_9}$ is; these processes have no energy barrier,[28,31] and (in the first approximation) the rate constant includes only entropy contributions.

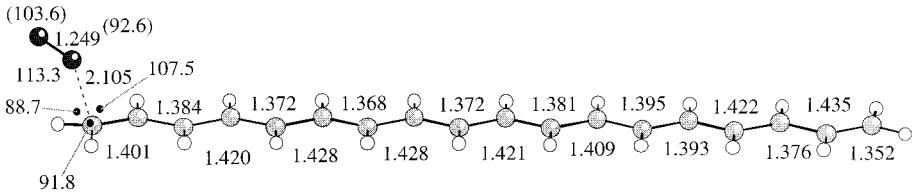


**Figure 11.** DFT optimized structure for the transition state **TS$_4$**. Bond lengths in Å; angles and dihedral angles (OOC/OCC and OCC/CCC are given in parentheses) in degrees.

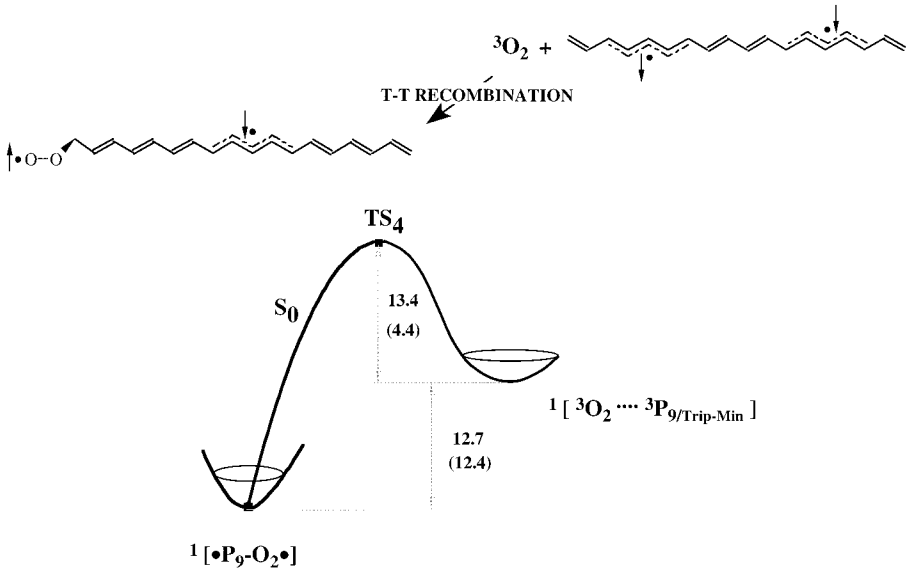


**Figure 12.** DFT energy profile (values in kcal mol$^{-1}$) for the triplet−triplet recombination process (see subsection **iv**). Values in parentheses represent spin-unprojected energies. The relative positions for the singlet (**S$_0$**) state of the triplet−triplet reactants, transition state (**TS$_4$**), and diradical product are shown.

range (see subsection **i**); thus, also in the case of the lower activation energy, the triplet−triplet recombination reaction seems to be a slower process. Nevertheless, the reaction must overcome an even higher barrier (13.4 kcal mol$^{-1}$ being its spin-projected value), and for this reason, we expect that this singlet-diradical formation pathway is very unfavored.

## 4. Conclusions

Carotenoids play an important role in the protective action of biological tissues, and a better understanding of the mechanisms of these processes is certainly desirable. In the present paper, we have investigated, using DFT methods, the reaction paths associated with the different reactions which occur between the oxygen molecule and a model carotenoid. Our results indicate that carotenoids can be involved in different types of reactions which include energy transfer, 1,2-addition, $T_1$ dissociation, and triplet−triplet recombination. These results and a summary of the corresponding reaction pathways are illustrated in Figure 13 (in Figure 14 we have summarized the results obtained for the shorter model system). It can be seen that the energy transfer process involves an almost barrierless path; therefore, this *catalytic* physical quenching (absent in the shorter system) is the most favored route. Nevertheless, secondary but concomitant low-energy barrier reactions appear to occur via the direct attack of the singlet-oxygen upon the double bonds of the carotenoid model. These processes lead to diradical systems where singlet and triplet states are degenerate. While ring-closure reactions on $S_0$ lead to the production of 1,2-addition dioxetane intermediates (which may then decompose to the final observed carbonyl chain cleavage oxidation products[11]), an efficient and competitive $S_0 \rightarrow T_1$ ISC may also occur at the diradical minima configuration, and deactivated triplet oxygen, together with the starting singlet ground-state carotene, is produced through a dissociation process on $T_1$. Singlet-diradical formation followed by ISC and triplet dissociation represent an alternative chemically mediated *catalytic* quenching of the singlet-oxygen which seems to be more favored than oxidation reactions. This alternative process may act, together with the more efficient physical pathway, to reduce competitive oxidation which results in the loss of carotenoids and thus of antioxidant protection. Our results suggest a reaction scheme for these processes (Scheme 2).

**Acknowledgment.** This research has been supported in part by the Access to Supercomputing Facilities for European Researchers project of the Training and Mobility of Researchers (contract ERBFMGECT950062 (DG-12 MEMO)) established between the European Community and CESCA/CEPBA.

**Supporting Information Available:** Tables which include the total energy values, the relative energies, and the $\langle S_2 \rangle$ values for *all-trans* linear polyenes $P_{11}$, $P_9$, and $P_3$, for the oxygen molecule, for the stationary points of the $P_9$ plus oxygen system, and for the stationary points of the $P_3$ plus oxygen system (3 pages print/PDF). See any current masthead page for ordering information and for web access instructions.

## Appendix. Some Calibration at Higher Levels of Theory: *all-trans* Hexatriene ($P_3$) + Singlet-Oxygen ($^1O_2$)

To test if the DFT approach is a suitable method for a reactivity study of an oxygen−polyene system, we have

(33) Triplet−triplet recombination (subsection **iv**) is a bimolecular process with a second-order rate constant $k$.[24] In this case, carotenoid lifetime ($\tau$) depends on the inverse of the pseudo first-order rate constant ($\tau = k^{-1}[^3O_2]^{-1}$) where a constant value of $10^{-3}$ M for $[^3O_2]$ is considered.[31]

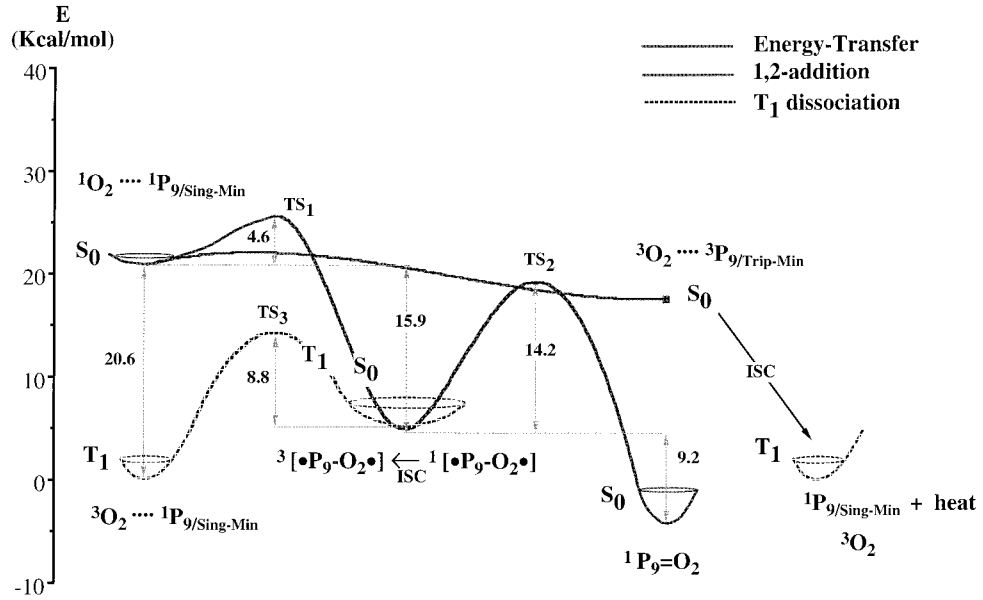


**Figure 13.** Summary of the DFT energy profiles (spin-projected values in kcal mol$^{-1}$) of the main reaction paths computed for the longer model system ($0_2$ + **P$_9$**). The relative positions of the triplet (**T$_1$**) and singlet (**S$_0$**) states of reactants, intermediates, products, and transition states (**TS$_1$**, **TS$_2$**, and **TS$_3$**) are shown.

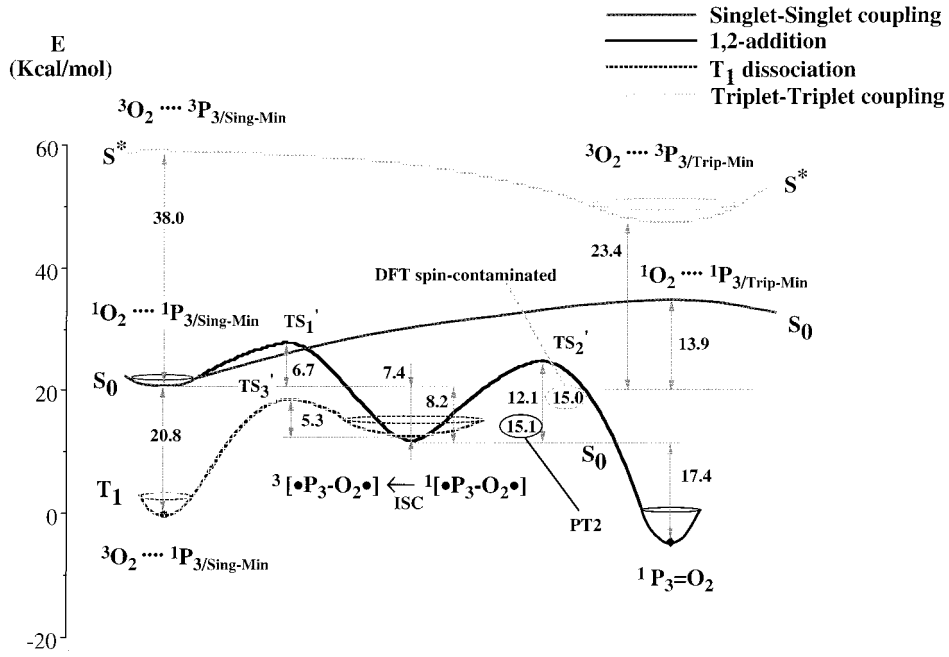


**Figure 14.** Summary of the DFT energy profiles (spin-projected values in kcal mol$^{-1}$) of all the reaction paths computed for the shorter system ($0_2$ + **P$_3$**). The shaded circled value represents the spin-unprojected energy barrier, while the other circled value is the PT2 energy barrier. The shaded line is associated with the triplet−triplet coupling description which represents the excited singlet (**S***) state. The relative positions of the triplet (**T$_1$**), singlet (**S$_0$**), and excited singlet (**S***) states of reactants, intermediates, products, and transition states (**TS$_1$′**, **TS$_2$′**, and **TS$_3$′**) are shown.

performed an analogous DFT investigation of the reaction mechanisms between the *all-trans* hexatriene (**P$_3$**) and the singlet-oxygen, reoptimizing some structures and recomputing some energy values at the CAS-SCF level[16] with PT2[14] correlation-energy correction. This system, with its 10 heavy atoms, is right at the limit for such types of computations (see Computational Details). Moreover, this shorter system enables us, first, to check (via DFT analytical frequency calculations) the nature of the optimized stationary points corresponding to those found in the longer system and, second, to investigate the differences in chemical reactivity between long-chain polyenes (such as carotenoids) and shorter conjugated chains toward the singlet-oxygen.

The results of this shorter system DFT study are summarized in Figure 14, and the energies are given in Table 3. The reaction pathways and their trends are almost the same for the two systems, and it was possible to localize and characterize (via frequency computations) the transition structures (**TS$_1$′**, **TS$_2$′**, **TS$_3$′**) and minima corresponding to the previously found 1,2-addition and $T_1$-dissociation processes (Figures 3c, 6c−d, 8c−d, and 9b). We know that a very high singlet-oxygen quenching efficiency has been observed for carotenoids[1,9] (Figure 1), and indeed, in the **$^1$P$_9$** + $^1O_2$ system, an energetically favored (almost barrierless) energy transfer path on $S_0$ (Figure 4) has been identified. On the other hand, short polyenes are not singlet-oxygen quenchers, and it was not possible to locate an $S_0$ energy

**Table 3.** B3LYP/6-31G* Relative Energies ($\Delta E$) and $\langle S^2 \rangle$ Values for the Stationary Points of the $\mathbf{P_3}$ Plus Oxygen System. The Weight ($\omega$) of the Reference Zero-Order CAS-SCF Wave Function in the First-Order Corrected PT2 Wave Function Has also Been Reported

| structures | state | $\langle S^2 \rangle$ | $\omega$ | $\Delta E^a$ |
|---|---|---|---|---|
| **S**−**S** complex | $(T_1)^b$ | 2.01 | | 0.0[e] |
| $O_2$···$\mathbf{P_{3/Sing\text{-}Min}}$ | $(S_0)^c$ | 1.00 | | 20.8 (10.4) |
| | $(S^*)^d$ | | | 58.8 |
| **T**−**T** complex | $(S_0)^c$ | 1.00 | | 34.7 (24.3) |
| $O_2$···$\mathbf{P_{3/Trip\text{-}Min}}$ | $(S^*)^d$ | 2.02 | | 44.2 |
| $\mathbf{TS_1}'$ | $(T_1)$ | 2.09 | | 17.9 |
| | $(S_0)$ | 1.05 | | 27.5 (22.7) |
| diradical-minimum | $(S_0)$ | 1.02 | | 12.6 (13.0) |
| | $(T_1)$ | 2.05 | | 13.4 |
| | $(S_0)^f$ | | 0.76 | 0.0 |
| | $(S_0)^g$ | | 0.77 | 0.0 |
| $\mathbf{TS_2}'$ | $(S_0)$ | 0.65 | | 24.7 (27.9) |
| | $(T_1)$ | 2.05 | | 35.0 |
| | $(S_0)^f$ | | 0.75 | 15.1 |
| | $(S_0)^g$ | | 0.75 | 15.7 |
| $\mathbf{TS_3}'$ | | 2.08 | | 18.7 |
| dioxetane minimum | $(S_0)$ | 0.00 | | −4.8 |

[a] When spin-projection is applied (see Computational Details and ref 17), the spin-contaminated values are reported in parentheses. [b] The triplet overall wave function refers to a triplet-oxygen plus singlet-polyene coupling. [c] The singlet overall wave function refers to a singlet-oxygen plus singlet−polyene coupling. [d] The singlet overall wave function refers to a triplet-oxygen plus triplet−polyene coupling. [e] Absolute energy (au) −383.718 87. [f] PT2 energy on the DFT optimized structure. [g] PT2 energy on the CAS-SCF optimized structure.

transfer path in the hexatriene−oxygen model. The triplet−triplet products of the hypothetical physical quenching (see Figure 14 and Table 3) are associated with the singlet excited state S*, and the two *diabatic* curves describing the singlet−singlet and triplet−triplet coupling never cross, in contrast to the behavior found in the longer system which gives rise to the energy transfer channel on $S_0$. Physical quenching is prevented, not because of a too high energy barrier but because it does not exist at all. In fact, the triplet−triplet coupling ($^3\mathbf{P_9}$···$^3O_2$) remains always localized on S*, and this is due to the larger singlet−triplet energy gap in short conjugated polyenes (see Table 1 for the computed energy values on the singlet $S_0$ minimum, $\mathbf{P_{3/Sing\text{-}Min}}$, and triplet $T_1$ minimum, $\mathbf{P_{3/Trip\text{-}Min}}$). As for the longer system, we have carried out computations for the triplet−triplet coupling (S* state) due to the intrinsic stability of the corresponding wave function (DFT wave function stability has been checked both in the singlet−singlet ($S_0$) and triplet−triplet (S*) states).

The structures of the diradical minimum and ring-closure transition state have been reoptimized at the CAS-SCF level,[16] and the energy barrier has been recomputed by single-point PT2[14] calculations to account for the dynamic correlation-energy correction (Figure 14 and Table 3). DFT and CAS-SCF optimized structures are compared in Figures 6d and 8c. Significant differences are observed in the O−O bond distance (respectively 1.321 and 1.297 Å for the diradical minimum, 1.405 and 1.364 Å for the dioxetane transition state). The same situation was observed comparing DFT and CAS-SCF optimized singlet-oxygen structures; the DFT O−O bond distance is longer than the CAS-SCF one (and the first one agrees very well with the available experimental value, see Figure 2b) probably because of a reduced component of the correlation-energy in the CAS-SCF wave function used during the optimization. This component could be important to obtain correct geometrical structures in oxygen-containing molecules since the correlation-energy contribution is quite important for geometries as well as for energies. The PT2 absolute energy is lower when computed at DFT geometries than when computed for CAS-SCF structures (see Supporting Information) so that DFT optimized structures are more accurate. In any case, both PT2 recomputed energy barriers (15.1 and 15.7 kcal mol$^{-1}$ for DFT and CAS-SCF optimized geometries, respectively) agree quite well with the DFT projected energy (12.1 kcal mol$^{-1}$) (a similar computational approach has been used successfully in a previous work,[18] and we think this level is sufficiently accurate for our investigation).

An interesting question may naturally arise from these results, i.e. how many double bonds are needed for the energy transfer process to exist, and how many for it to become efficient with respect to the other chemical (oxygen addition) pathways. An answer just based on the results for the short and long systems presented in this paper is certainly not conclusive. From the energies computed on the small $^1\mathbf{P_3}$ + $^1O_2$ system (see Figure 14), we know that shifting the two *diabatic* curves (describing the singlet−singlet and triplet−triplet couplings) one to the other of only 9.5 kcal mol$^{-1}$ will result in a crossing and possibly in the existence of an energy transfer (even though not efficient) process. We guess this may happen from 5 or 6 conjugated double-bond polyenes; however, for a competitive physical quenching, the singlet−singlet $S_0$ and triplet−triplet S* states have to be very close to each other already at the reactant FC region since this condition is needed to have a sudden crossing and prevent a significant energy barrier (this simply means that the singlet−triplet energy gap for the polyene has to be as close as possible to that of $0_2$). Since a barrier (even if very small indeed) is still observable along the interpolated path of our $\mathbf{P_9}$ model system (see Figures 4 and 13), we guess that 8 (or at most 9) is the minimum number of conjugated double bonds in a polyene for energetically favored energy transfer to take place.

JA9805270